nature microbiology

SUPPLEMENTARY INFORMATION

https://doi.org/10.1038/s41564-020-0717-x

In the format provided by the authors and unedited.

General quantitative relations linking cell growth and the cell cycle in *Escherichia coli*

Hai Zheng[1,2,5], Yang Bai[1,5], Meiling Jiang[1,5], Taku A. Tokuyasu[1], Xiongliang Huang[1,2], Fajun Zhong[1], Yuqian Wu[1], Xiongfei Fu[1,2], Nancy Kleckner[3], Terence Hwa[4] and Chenli Liu[1,2] ✉

[1]CAS Key Laboratory for Quantitative Engineering Biology, Shenzhen Institute of Synthetic Biology, Shenzhen Institutes of Advanced Technology, Chinese Academy of Sciences, Shenzhen, People's Republic of China. [2]University of Chinese Academy of Sciences, Beijing, People's Republic of China. [3]Department of Molecular and Cellular Biology, Harvard University, Cambridge, MA, USA. [4]Department of Physics, University of California, San Diego, La Jolla, CA, USA. [5]These authors contributed equally: Hai Zheng, Yang Bai, Meiling Jiang. ✉e-mail: cl.liu@siat.ac.cn

SUPPLEMENTARY INFORMATION

General quantitative relations linking cell growth and the cell cycle in *Escherichia coli*

Hai Zheng[1,2,*], Yang Bai[1,*], Meiling Jiang[1,*], Taku A. Tokuyasu[1], Xiongliang Huang[1,2], Fajun Zhong[1], Yuqian Wu[1], Xiongfei Fu[1,2], Nancy Kleckner[3], Terence Hwa[4], Chenli Liu[1,2,+]

[1]CAS Key Laboratory for Quantitative Engineering Biology, Shenzhen Institute of Synthetic Biology, Shenzhen Institutes of Advanced Technology, Chinese Academy of Sciences, Shenzhen 518055, People's Republic of China
[2]University of Chinese Academy of Sciences, Beijing 100049, People's Republic of China
[3]Department of Molecular and Cellular Biology, Harvard University, Cambridge, MA 02138, USA
[4]Department of Physics, U.C. San Diego, La Jolla, CA 92093-0374, USA

*equal contribution
[+]To whom correspondence may be addressed. Email: cl.liu@siat.ac.cn

Supplementary Notes

Summary

This supplement describes technical details of the model introduced in the main text, which we term the deterministic integral threshold model. We begin with a short review of cell cycle coordination based on the SMK growth law and the Donachie relations (**Sec. 1)**, which provides important background for understanding the significance of our results. The downfall of these older relations suggests a search for new conceptual foundations, constrained by the growth laws proposed here. We develop an accumulation-type model to begin this exploration (**Sec. 2**). A stochastic extension is described in **Sec. 3** and compared briefly to experimental data. The deterministic model is then placed in the context of related models and compared to a recently proposed model (**Sec. 4**). In the last section (**Sec. 5**), the stochastic model is applied to cell division during growth transitions, and the behaviors obtained are compared to the well-known 'rate maintenance' phenomenon.

1. Classic understanding of coordination

Classic understanding of the coordination of cell mass growth, chromosome replication, and cell division in bacterial is manifested by the empirical growth law of Schaechter-Maaløe-Kjeldgaard (SMK)[1] and the constant initiation mass hypothesis by Donachie[2]. This framework states the followings for steady state cells in the fast-growth regime, i.e. doubling time shorter than 1 hour:

1) average cell mass depends exponentially on growth rate[1];

2) the time interval *C*, from initiation to termination of one round of DNA replication, and *D*, from replication termination to corresponding cell division, sum to a constant[3];

3) the "initiation mass" (cellular mass per replication origin at the time of replication initiation) is constant[2].

Bremer *et al*[4], among others, have noted that the average number of origins per cell is

$$\bar{o} = 2^{\frac{C+D}{\tau}} = e^{\lambda(C+D)}. \quad \text{(S1)}$$

A growth rate dependent $C+D$ results in a growth rate-dependent average mass per origin (m_{po}) as $m_{po} = \bar{m}(\lambda)/e^{\lambda(C+D)}$. The SMK growth law as reformulated by Donachie specifies that $\bar{m} \propto e^{\lambda(C+D)}$, and the growth rate dependence in m_{po} cancels out. As the initiation mass m_i is simply proportional to m_{po}, i.e. $m_i = m_{po}/\ln(2)$,[5] the SMK growth law implies constant initiation mass, independent of growth rate. The above three statements form a self-consistent theoretical framework in the quantitative description of cell division.

This classic framework provides the foundation for most recent theoretical work. For example, the models proposed by Ho *et al*.[6], and Micali *et al*.[7,8] used the assumption of constant initiation mass. One can save these models by applying the experimentally measured growth rate dependent initiation mass (given after **Eq. 2** in the main text), but its complex form complicates the biological interpretation. Instead, this opens up the search for new conceptions that can replace those such as the constant initiation mass and help illuminate how the cell manages the cell cycle.

2. The integral threshold model

Our model starts from the assumption that a cell accumulates a licensing product $L(t)$ produced by certain protein, with copy number $z(t)$ per cell, at a specific production rate r per protein. The protein $z(t)$ is assumed to have a constant concentration over time so that its copy number is proportional to cell mass, i.e., $z(t) = [z] \cdot m(t) = [z] \cdot m_b e^{\lambda t}$, where t is the time since the last division and $[z]$ is the cellular concentration of z. Like most proteins in balanced exponential growth, we assume $[z]$ is time-independent. We choose to use the protein abundance interpretation in this article as it is more biologically reasonable. The bacterium divides when the licensing product accumulation $L(t)$ passes a threshold L_c. Cell division is presumed to reset $L(t)$ to zero and distribute protein z equally into daughter cells. The licensing product accumulation can hence be written as

$$L(t) = \int_0^t r \cdot z(s) ds \,. \tag{S2}$$

Integrating the equation we get

$$L(t) = \frac{r}{\lambda}[z] \cdot (m(t) - m_b), \tag{S3}$$

where m_b is the birth mass. As cells divide when $L(t) = L_c$, we may calculate explicitly the division mass m_d,

$$m_d = L_c \frac{\lambda}{r[z]} + m_b \,. \tag{S4}$$

The added mass $\Delta m = m_d - m_b = L_c \frac{\lambda}{r[z]}$ is independent of the birth mass, so that the adder principle is obvious.

In the steady state of a deterministic dynamical process with symmetric division, we expect constant birth mass and division mass over all division cycles. So we have $m_d = 2m_b$. It is known that the population-averaged cellular mass $\overline{m}$ is proportional to population-averaged division mass $\overline{m_d}$ (for this deterministic process, $\overline{m_d} = m_d$) with a factor of ln2 in a steady state batch culture $\overline{m} = \ln 2 \cdot \overline{m_d}$ [9]. We then get for the average cell mass,

$$\overline{m} = 2 \ln 2 \, L_c \cdot \frac{\lambda}{r} \cdot [z] \,. \tag{S5}$$

Comparing to the relation between mass and growth rate (**Eq. 2**), we see that the growth-rate dependence of $\overline{m}$ can be most parsimoniously obtained if L_c is growth-rate independent, the production rate r is proportional to $1/(C+D)$ and m_0 is proportional to $1/(L_c[z])$. The dynamics of the accumulator thus takes the form

$$L(t) = \int_0^t \frac{1}{C+D} \cdot \frac{m(s)}{m_0} ds\,. \tag{S6}$$

We simulated the dynamics of the integral threshold model with a variety of initial cell masses. Cell masses quickly converged to the same dynamics around the expected steady-state cell mass (**Supplementary Fig. 3**), demonstrating the cell size control property of the model. We also confirmed that the simulation reproduces the linear relation (**Eq. 2**) with the same constant L_c for all growth rates (**Supplementary Fig. 4a**), as expected.

As noted in the main text, our empirical finding that $C = b(C+D)$, with $b \approx 0.625$, allows **Eq. 2** to be replaced with $\overline{m} = m_0' \cdot \lambda C$. Comparing this with **Eq. S5**, we can assign prefactor values $r = \frac{1}{C}$ and $m_0' = m_0/b$. Equivalently, using $D = (1-b)(C+D)$ we can assign prefactor values $r = \frac{1}{D}$ and $m_0'' = \frac{m_0}{1-b}$. Simulation using either set of prefactors results in the corresponding linear relations of average cell mass (see **Supplementary Fig. 4bc**), as expected. The pseudo code of the stochastic version provided in **Sec. 3** below, minus the parts that refer to the stochastic process, can be referred to as a guide for the simulation of this deterministic model.

3. Integral threshold model with noise

As any biological process experiences noise, we now consider a stochastic extension of the deterministic model described in **Sec. 2**. For simplicity, we model the noise as arising from fluctuations in the accumulation rate of the licensing product. As in the deterministic model, we assume cell division occurs when the licensing product $L(t)$ reaches a threshold L_c. After cell division, the licensing product experiences a renew process($L(t) = 0$). Within a cell division cycle, the cell mass and licensing product follow the dynamics as:

$$\frac{1}{\frac{m(t)}{m_0}} dL(\mathrm{t}) = \frac{1}{C+D} dt + \sqrt{2}\varepsilon \cdot d\Delta(t) \tag{S7}$$

where $\Delta(t)$ is a Gaussian white noise, such that $\langle \Delta(t) \rangle = 0, \langle \Delta(t)\Delta(t') \rangle = \delta(t-t')$. The parameter ε controls the noise levels of the stochastic process. We numerically simulated the dynamics of each bacterium in a mother machine setup, where only one daughter cell after cell division is kept. The pseudo code for the simulation is presented below.

Pseudo code :

Variables

N : cell number, 10^5 cells simulated in the mother machine set up, in unit 1

m : cellular mass, initial value = 1 if not defined, in unit OD_{600}·ml/10^9 cells

L : the accumulator, initial value = 0 if not defined, in a. u.

Δ : Gaussian random variable, mean value =0, standard deviation=1, in a. u.

Parameters

$dt = 0.01$: simulation time step, in unit mins

λ : growth rate, in unit $mins^{-1}$

$C + D$: time from DNA replication initiation to division, from **Eq. 1**, in unit mins

$\varepsilon = 0.01$: noise level, fitted value to distribution data.[10] [11], in unit $mins^{-0.5}$

$L_c = \frac{1}{2\ln 2} \approx 0.72$: threshold of $L(t)$, deduced in **Sec. 2**.

While $t < t_{max}$ **do**

cell mass growth

$m = m + \lambda \cdot m \cdot dt$

increase of the accumulation

Draw a random unit Gaussian variable Δ

$L = L + \frac{m}{m_0} \cdot \frac{1}{C+D} \cdot dt + \frac{m}{m_0} \cdot \sqrt{2}\varepsilon \cdot \sqrt{dt} \cdot \Delta$

cell divide if a threshold is passed

If $L \geq L_c$

$N = N + 1$: cell number increase

$m = m/2$: reset cell mass

$L = 0$: reset the accumulator

end

end

The birth mass, division mass, and doubling time distributions obtained for different growth rates were found to approximately overlap when rescaled by their respective averages, but they did not collapse to a single curve. An empirical scaling property of cell division was claimed by Taheri-Araghi *et al.*[11] and appears to also roughly hold for the data of Wallden *et al.*[10] (although not reported by those authors). Fitting the single parameter ε to the value 0.01, the simulations obtained workable fits to all three

empirical distributions, i.e. rescaled birth mass, division mass, and inter-division time (**Supplementary Fig. 5**).

The lack of correlation between birth mass and added mass, now called the adder phenomenon, is another important feature observed in cell division control. The deterministic version of the model is an adder model by construction (**Sec. 2**). We also confirmed numerically with the stochastic version that the added mass is uncorrelated to birth mass, while the inter-divison time and division size are correlated to birth mass (**Supplementary Fig.6**).

4. Comparison with previous models

Our integral threshold model belongs to a class of what can be termed "accumulator" models[12-15], in which some product or marker of cell cycle progression accumulates to a threshold value and then triggers or licenses cell division. Among these models, Si *et al.*[13] recently proposed (as an example) the complete Z-ring to be considered as the licensing product of cell division. This requires the number of FtsZ proteins per cell to reach a threshold. In a sense, our model can be viewed as an extension of this model of Si *et al*, but differs from theirs by emphasizing the growth-rate dependence (which they do not consider at all). We denote what would be the number of FtsZ proteins per cell as $X(t)$. In Si *et al*'s model, this quantity would increase with cell size $m(t)$ as

$$\frac{dX}{dt} = c \times \frac{dm}{dt}, \tag{S8}$$

where c is the concentration of FtsZ. This leads to $X(t) = X(0) + c \cdot [m(t) - m(0)]$, and cell division is licensed when $X(t)$ reaches a threshold X_0. To facilitate comparisons with our model, we rewrote **Eq. S8** as

$$X(t) = \int_0^t c \times \lambda m(s) ds \; + X(0), \tag{S9}$$

with $\frac{dm}{dt} = \lambda m(t)$ for exponentially growing cells.

Comparing **Eq. S9** to **Eq. S2** of our model, we see that the two models has the same mathematical for, with the number abuandance $z(s)$ given by $c \cdot m(s)$, or with c being $[z]$. There are two differences: 1) the production rate of the licensing product is proportional to the cell mass growth rate λ in Si et al's model, while it is $1/(C + D)$ in our model; 2) $X(t)$ is reset to its birth value $X(t = 0)$ instead of 0 in our model. The first difference makes the two models biologically distinct: In the model of Si *et al.*, FtsZ protein and its product (the Z-ring) are interchangeable, whereas in our model the two are distinct. Regarding the second difference, the definition of L can be easily modified to include a nonzero reset value, while yielding the same division behavior.

In summary, both the model of Si *et al.* and ours consider cell division as a mass-dependent process instead of being licensed directly by DNA replication events such as initiation. The main difference is that we introduced a specially chosen growth-rate dependent synthesis (accumulation) rate, $r = 1/(C + D)$ which recovers the linear cell mass relation (**Eq. 2** of the main text). Si *et al*.[13] did not attempt to model the growth rate-dependence of the average cell mass, and would need to invoke other growth-rate dependence processes in order to do so.

As the synthesis rate r in our integral-threshold model explicitly connects DNA chromosome replication/segregation with cell division, our model can also be discussed in the context of the "concurrent model" proposed by Micali *et al.*[8]. The latter model assumes that the cell division control depends on both DNA replication and mass accumulation. They explored an intriguing possibility that DNA replication-segregation and construction of cell division machinery proceeded independently, with cell division determined by the slowest process in a given cell. Our model suggests that these two processes are linked via a licensing product accumulation process, of which the synthesis rate is proportional to $1/C$, or $1/D$, or $1/(C + D)$, i.e., the rate of DNA elongation, or the rate of chromosome segregation, or their combination. Our integral threshold model thus suggests a path of how potentially the 'accumulator' and concurrent models may be unified.

5. Cell division during growth transition

As the integral threshold model captures the linear relation of average cellular mass in steady state, we next extend this model to check how it behaves during growth transitions. 'Rate maintenance' is an important phenomenon that occurs when bacteria are transferred from a slow-growth medium to a fast-growth medium[16]. It is observed that while the rate of cell mass growth changes rapidly to the rate of post-shift growth, the rate of cell number growth is *maintained* at that of pre-shift growth for certain period. This phenomenon is often considered as strongly supporting a link between chromosome replication and cell division[17].

Here we apply the stochastic integral threshold model as defined in **Sec. 3** to predict the transition dyanmics between different growth rates. We take the mass growth rate $\lambda_m(t)$ to be a linear fit of the observed transition during nutrition shift-up from growth media M25 to M6 (**Supplementary Fig. 7a**). The time-dependent C+D is then derivable from **Eq. 2** (purple curve in **Supplementary Fig. 7a**). The model is first simulated at the pre-shift growth condition until a quasi-steady state mass distribution was achieved. Batch culture condition was applied where the both daughter cells were kept and cell number increases accordingly. Then by random sampling 10^4 cells from this mass distribution as the initial condition, we restart the simulation with pre-shift growth rate and perform growth rate transition as described above.

The cell number growth curve exhibits a pronounced horizontal shift relative to the mass growth curve, reminiscent of the rate-maintenance phenomenon (**Supplementary Fig. 7b**). However, it is difficult to fully capture the instantaneous cell number growth rate (**Supplementary Fig. 7c**) and the average cell mass data (**Supplementary Fig. 7d**). Instead of a firm 'maintenance' of cell number growth rate, our

model predicts a smooth transition of cell number growth rate after medium shift. A more detailed model may thus be necessary to recapture the classic rate-maintainance phenomenon. A potential solution would be to incorporate chromosomal events in a more direct manner, as ‘rate maintenance’ strongly suggests a causal link between chromosome replication and cell division. We leave this to future investigations.

Supplementary Figures

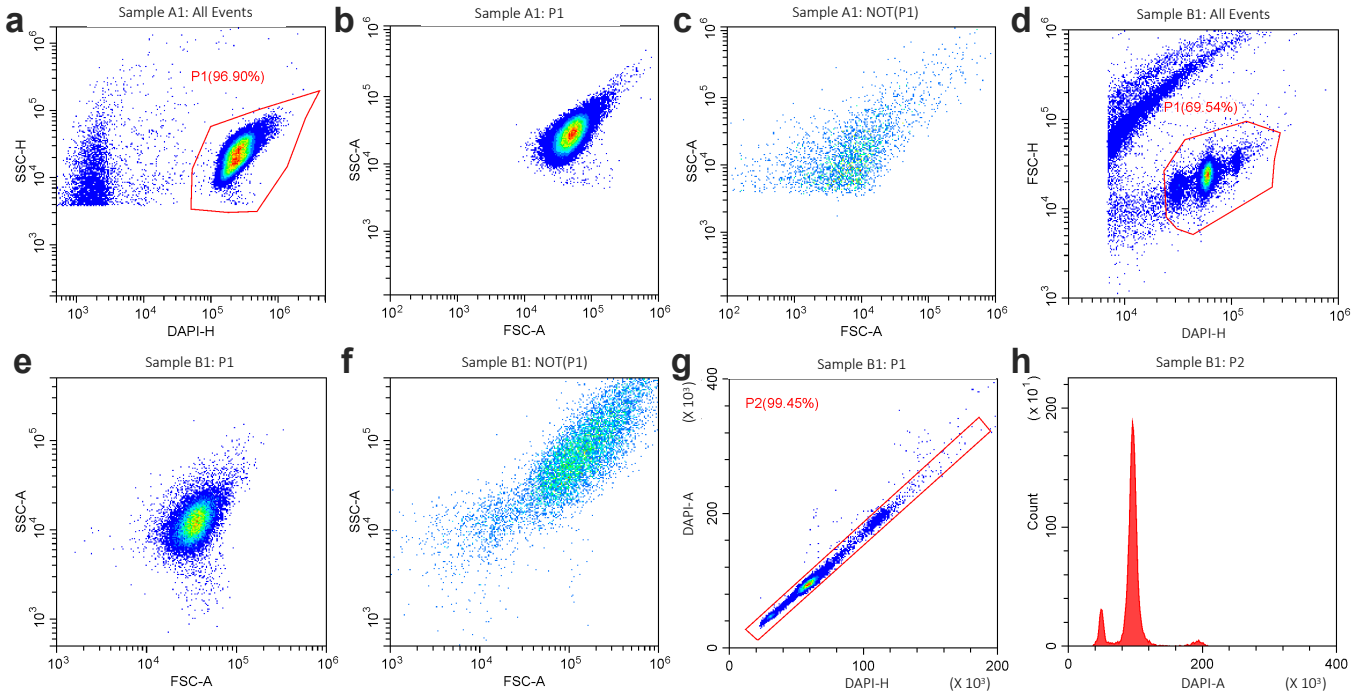

Supplementary Figure 1 | Gating strategy used in flow cytometry analysis. a-c, Gating strategy used in cell counting and FSC characterization experiments. Particles in P1 in panel **a** were regarded as the bacterial cells. The FSC-A/SSC-A plots for P1 or outside P1 sub-populations are shown in panels **b** or **c**, respectively. **d-h**, Gating strategy used in experiments for population-averaged cellular oriC characterization. Particles in P1 in panel **d** were regarded as the bacterial cells. The FSC-A/SSC-A plots for P1 or outside P1 sub-populations are shown in panels **e** or **f**, respectively. A further gate was set on P1 to eliminate non-single-cell particles (**g**). **h**, The DAPI-A histogram for particles in P2 was used for calculating the population-averaged *oriC* number.

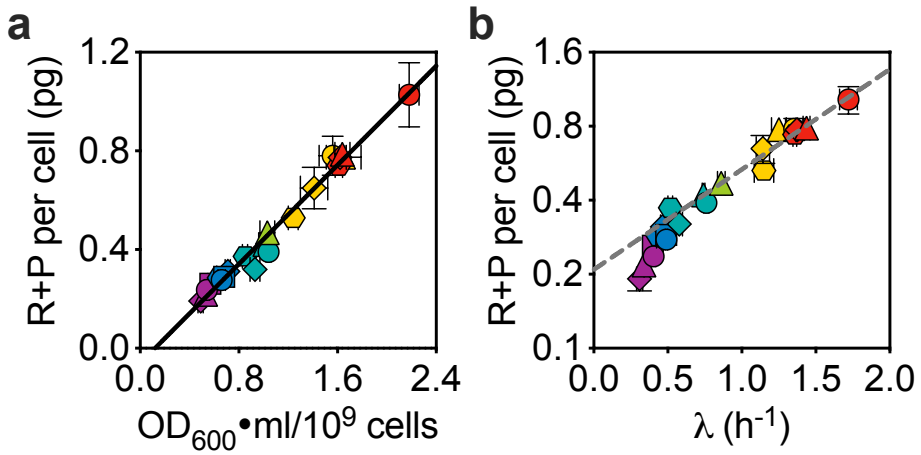

Supplementary Figure 2 | Relationship between the sum of RNA and protein per cell and growth rate. a, The combined mass of RNA and protein per cell is linearly correlated with the OD_{600}·ml per cell. **b,** When plotted against growth rate, the combined mass of RNA and protein per cell closely resemble the trends exhibited by other measures in **Fig. 1a-d**. Symbols and error bars represent the mean±SDs of the data. Sample size and mean value for each symbol are provided in **Extended Data Fig. 8.**

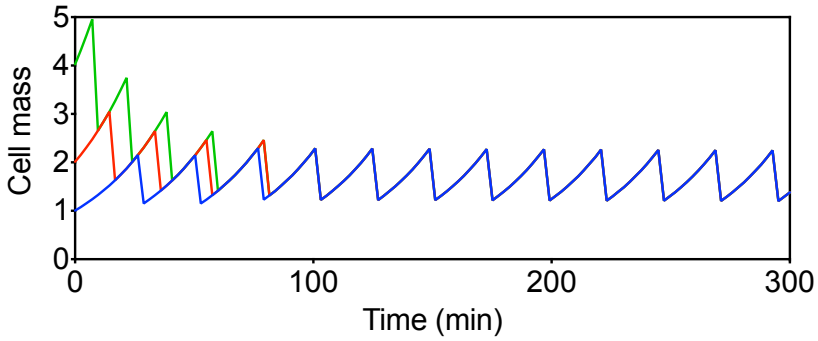

Supplementary Figure 3 | Steady state dynamics implied by Eq. S6 are independent of initial condition. Simulation of single cells having different initial cell masses ($m_b = 1, 2, 4$) in the integral threshold model. Doubling time is 24 min, and cell mass is in unit of OD_{600}·ml per 10^9 cells. Similar results were obtained for all growth rates tested (data not shown).

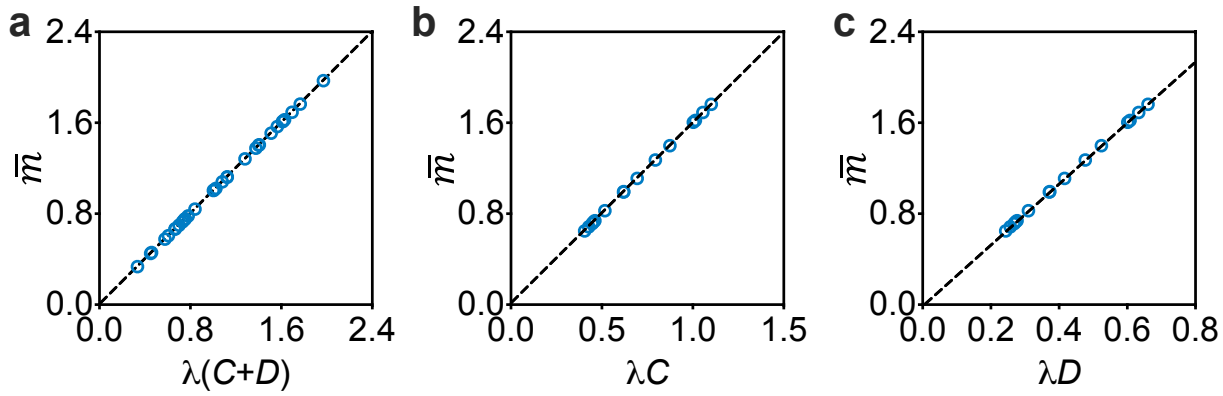

Supplementary Figure 4 | Validation of the linear relation of the average cell mass described by the simulations. The average cell mass (in unit of OD_{600}·ml per 10^9 cells) calculated by $\bar{m} = \ln 2 \cdot m_d$ is plotted with respect to $\lambda(C + D)$ **(a)**, λC **(b)**, and λD **(c)**. m_d is the division mass of steady state single cells in the simulations. The dashed line represents the linear relations **Eq. 2 (a),** $\bar{m} = m_0' \cdot \lambda C$ **(b)**, and $\bar{m} = m_0'' \cdot \lambda D$ **(c)**.

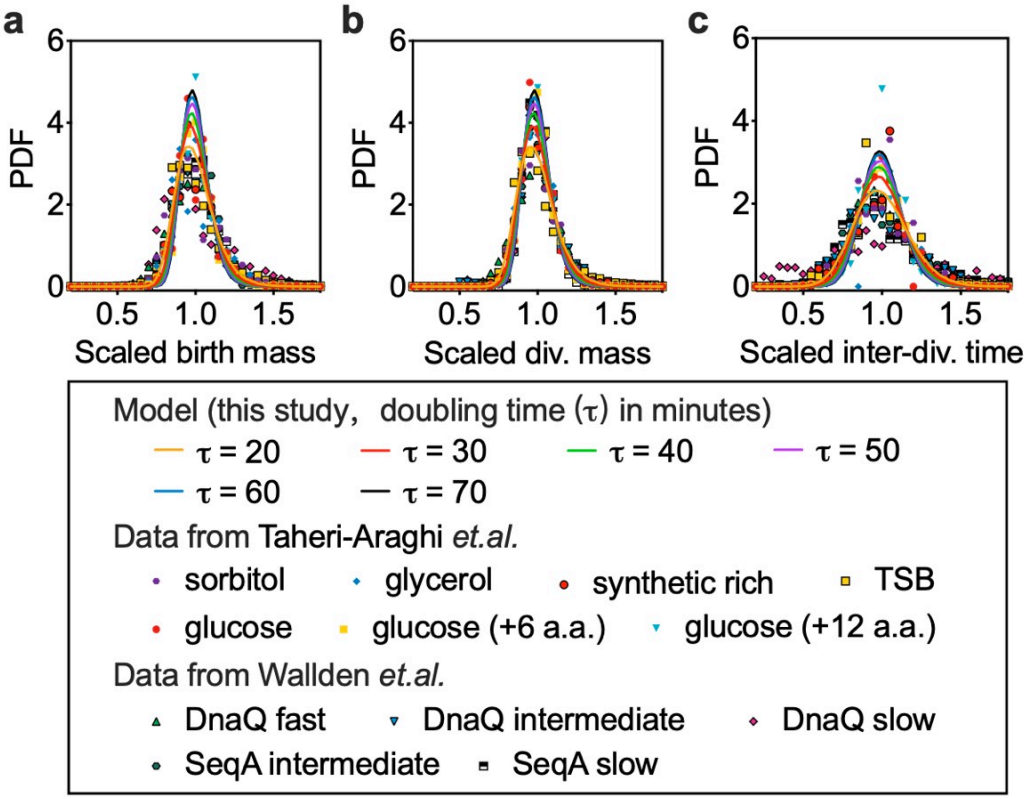

Supplementary Figure 5 | Simulations of cell size distributions. Normalized cell birth mass **(a)** division mass **(b)** and inter-division time **(c)** distributions of simulations of different growth rates (lines of different colors) were compared to the rescaled experimental data from Taheri-Araghi *et al*.[11] and Wallden *et al.*[10] (data of cell volume is regarded as cell mass).

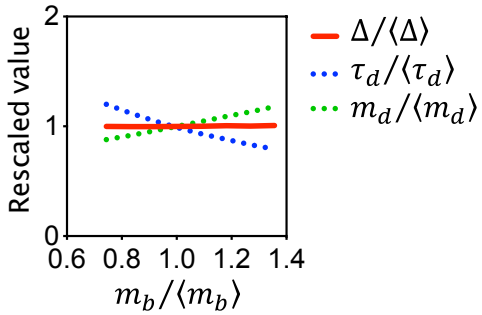

Supplementary Figure 6 | Simulations captured the adder phenomenon. Rescaled bulk averaged added mass (red), interdivision time (blue), and division mass (green) were plotted against rescaled birth mass. Only the added mass was found independent to birth mass. The growth rate was set as 0.92 h^{-1}. Similar results were observed across entire spectrum of growth rates (data not shown).

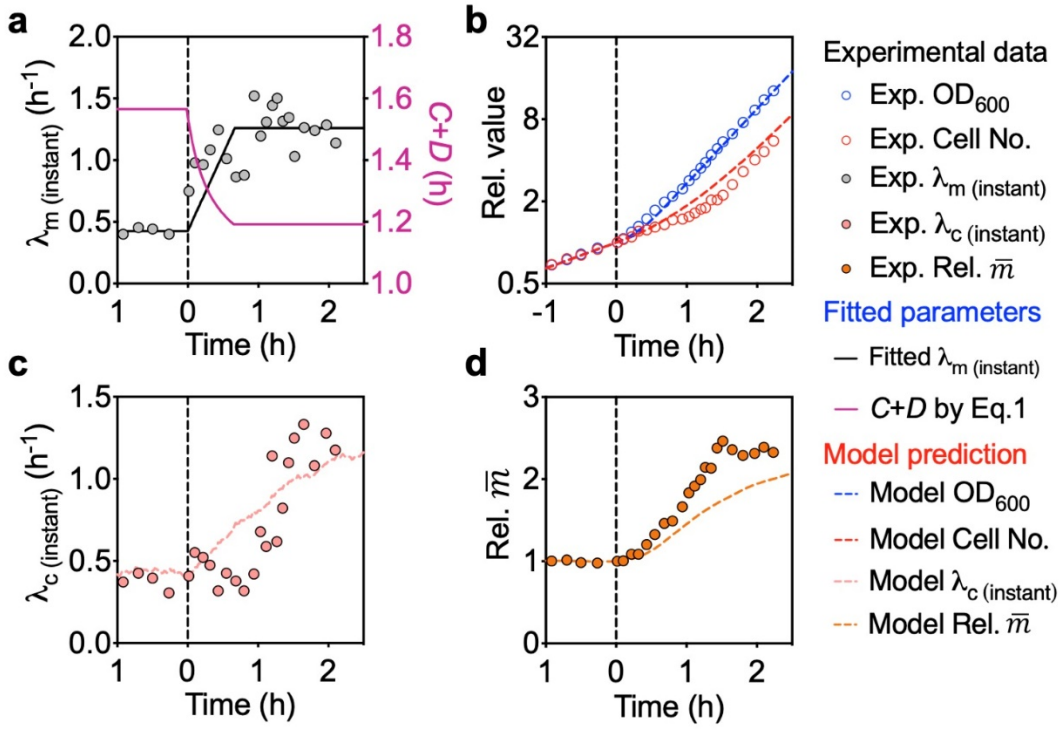

Supplementary Figure 7 | Simulations of the stochastic integral threshold model show delay in cell number growth rate during nutrition shift-up experiment. a. Nutrition shift-up experiment was performed with a shift in growth media from M25 to M6 at time 0 while following OD_{600} (blue circles) and cell number (red circles). In the simulation, the total cell mass growth rate dynamics was fitted according to a "ramp" fit to the transition in empirical mass growth rates. The dynamics of the growth rate during transition was fit by a simple linear function connecting the two time-invariant steady state growth rates, using a least-squared fit of the time while the time-dependent value of $C+D$ was calculated by **Eq. 2** (purple line). **b**. The cell number growth curve exhibits a pronounced shift relative to the mass growth curve, with a scale set by $C+D$, reminiscent of the rate-maintenance phenomenon. **c**. The stochastic integral threshold model is insufficient to predict the dynamics of cell number growth rate as it predicts smoothly increasing growth rate λ_c, while the experimental growth rate shifts during a short period from one state to another. **d**. The experimental data shows that $\bar{m}$ reaches the new steady-state value faster than predicted by the model.

Supplementary Tables

1. Chemical composition of the buffer and supplements for growth media

	Chemical compound	Final conc.	Notes
MOPS Buffer (PH 7.4)	MOPS	40 mM	Adjust to PH=7.4
	Tricine	4 mM	
	$FeSO_4$	10 μM	
	NH_4Cl	9.5 mM	
	K_2SO_4	0.276 mM	
	$CaCl_2$	0.5 μM	
	$MgCl_2$	0.525 mM	
	NaCl	50 mM	
	$(NH_4)_6Mo_7O_{24}$	3 nM	Micronutrient
	H_3BO_3	0.4 μM	Micronutrient
	$CoCl_2$	30 nM	Micronutrient
	$CuSO_4$	10 nM	Micronutrient
	$MnCl_2$	80 nM	Micronutrient
	$ZnSO_4$	10 nM	Micronutrient
	K_2HPO_4	1.32 mM	
M9 Buffer	Na_2HPO_4	47 mM	
	KH_2PO_4	22 mM	
	NaCl	8.5 mM	
	NH_4Cl	18.7 mM	
	Thiamine HCl	1 mM	
	$MgSO_4$	2 mM	
	$CaCl_2$	0.1 mM	
EZ	Alanine	0.8 mM	
	Arginine	5.2 mM	
	Asparagine	0.4 mM	
	Aspartic acid	0.4 mM	
	Cysteine	0.1 mM	
	Glutamic acid	0.6 mM	
	Glutamine	0.6 mM	
	Glycine	0.8 mM	
	Histidine	0.2 mM	
	Isoleucine	0.4 mM	
	Leucine	0.8 mM	
	Lysine	0.4 mM	
	Methionine	0.2 mM	
	Phenylalanine	0.4 mM	
	Proline	0.4 mM	

	Serine	10 mM	
	Threonine	0.4 mM	
	Tryptophan	0.1 mM	
	Tyrosine	0.2 mM	
	Valine	0.6 mM	
	Thiamine HCl	10 µM	Vitamin
	Calcium pantothenate	10 µM	Vitamin
	p-aminobenzoic acid	10 µM	Vitamin
	p-hydroxybenzoic acid	10 µM	Vitamin
	2,3-dihydroxybenzoic acid	10 µM	Vitamin
20 AA	Alanine	0.8 mM	
	Arginine	5.2 mM	
	Asparagine	0.4 mM	
	Aspartic acid	0.4 mM	
	Cysteine	0.1 mM	
	Glutamic acid	0.6 mM	
	Glutamine	0.6 mM	
	Glycine	0.8 mM	
	Histidine	0.2 mM	
	Isoleucine	0.4 mM	
	Leucine	0.8 mM	
	Lysine	0.4 mM	
	Methionine	0.2 mM	
	Phenylalanine	0.4 mM	
	Proline	0.4 mM	
	Serine	10 mM	
	Threonine	0.4 mM	
	Tryptophan	0.1 mM	
	Tyrosine	0.2 mM	
	Valine	0.6 mM	
11 AA	Alanine	0.8 mM	
	Arginine	5.2 mM	
	Asparagine	0.4 mM	
	Aspartic acid	0.4 mM	
	Glutamic acid	0.6 mM	
	Glutamine	0.6 mM	
	Glycine	0.8 mM	
	Proline	0.4 mM	
	Serine	10 mM	
	Threonine	0.4 mM	
	Cysteine	0.1 mM	
	Histidine	0.2 mM	

9AA	Isoleucine	0.4 mM	
	Leucine	0.8 mM	
	Tryptophan	0.1 mM	
	Valine	0.6 mM	
	Lysine	0.4 mM	
	Methionine	0.2 mM	
	Phenylalanine	0.4 mM	
	Tyrosine	0.2 mM	
CAA	Casamino acids	0.2% (w/v)	
AUCG	Adenine	0.2 mM	
	Cytosine	0.2 mM	
	Uracil	0.2 mM	
	Guanine	0.2 mM	

Remarks:

The composition of the MOPS buffer, EZ, and AUCG are based on Neidhardt Supplemented MOPS Defined Medium, prepared as described on the University of Wisconsin-Madison *E.coli* Genome Project website. The concentration for each amino acid used in 20 AA, 11 AA, 9 AA is identical to that used in EZ. The composition of M9 buffer and CAA are kept in accordance with the protocol presented on the OpenWetWare website.

2. Summary of quantities

Measured quantities	Definitions	Methods
$\overline{m}$	Average cellular mass	See Methods
$\bar{o}$	Average *OriC* number per cell	See Methods
C	Time to replicate one chromosome	See Methods
Fitting parameters		
λ_m	Cell mass growth rate in batch culture	Exponential fitting of the cell mass (OD_{600}) growth curve
λ_c	Cell number growth rate in batch culture	Exponential fitting of the cell number growth curve
α, β	Fitting parameters of **Eq. 1**, **Fig. 2a**	Best fit with least square method $R^2 > 0.97$
m_0	Fitting slope of **Eq. 2**, **Fig. 4a**	Best fit with least square method $R^2 > 0.97$
m_0'	Fitting slope in **Extended Data Fig. 7b**	Best fit with least square method $R^2 > 0.94$
b	Fitting slope of **Extended Data Fig. 7a**	Best fit with least square method $R^2 > 0.94$
Deduced quantities		
$T = C + D$	Time required from DNA replication initiation to the first cell division after its termination	Deduced from $C + D = ln(\bar{o})/\lambda$ see Methods
m_i	Initiation mass	Deduced from $m_i = \overline{m}/(\bar{o} \cdot ln2)$[5]

Supplementary References

1 Schaechter, M., Maaloe, O. & Kjeldgaard, N. O. Dependency on medium and temperature of cell size and chemical composition during balanced grown of Salmonella typhimurium. *J Gen Microbiol* **19**, 592-606, doi:10.1099/00221287-19-3-592 (1958).

2 Donachie, W. D. Relationship between cell size and time of initiation of DNA replication. *Nature* **219**, 1077-1079, doi:10.1038/2191077a0 (1968).

3 Cooper, S. & Helmstetter, C. E. Chromosome replication and the division cycle of Escherichia coli B/r. *J Mol Biol* **31**, 519-540, doi:10.1016/0022-2836(68)90425-7 (1968).

4 Bremer, H. & Churchward, G. An examination of the Cooper-Helmstetter theory of DNA replication in bacteria and its underlying assumptions. *J Theor Biol* **69**, 645-654, doi:10.1016/0022-5193(77)90373-3 (1977).

5 Bremer, H., Churchward, G. & Young, R. Relation between growth and replication in bacteria. *J Theor Biol* **81**, 533-545, doi:10.1016/0022-5193(79)90051-1 (1979).

6 Ho, P. Y. & Amir, A. Simultaneous regulation of cell size and chromosome replication in bacteria. *Front Microbiol* **6**, 662, doi:10.3389/fmicb.2015.00662 (2015).

7 Micali, G., Grilli, J., Marchi, J., Osella, M. & Cosentino Lagomarsino, M. Dissecting the Control Mechanisms for DNA Replication and Cell Division in E. coli. *Cell Rep* **25**, 761-771 e764, doi:10.1016/j.celrep.2018.09.061 (2018).

8 Micali, G., Grilli, J., Osella, M. & Cosentino Lagomarsino, M. Concurrent processes set E. coli cell division. *Sci Adv* **4**, eaau3324, doi:10.1126/sciadv.aau3324 (2018).

9 Bremer, H. & Dennis, P. P. Modulation of Chemical Composition and Other Parameters of the Cell at Different Exponential Growth Rates. *EcoSal Plus* **3**, doi:10.1128/ecosal.5.2.3 (2008).

10 Wallden, M., Fange, D., Lundius, E. G., Baltekin, O. & Elf, J. The Synchronization of Replication and Division Cycles in Individual E. coli Cells. *Cell* **166**, 729-739, doi:10.1016/j.cell.2016.06.052 (2016).

11 Taheri-Araghi, S. *et al.* Cell-size control and homeostasis in bacteria. *Curr Biol* **25**, 385-391, doi:10.1016/j.cub.2014.12.009 (2015).

12 Ghusinga, K. R., Vargas-Garcia, C. A. & Singh, A. A mechanistic stochastic framework for regulating bacterial cell division. *Sci Rep* **6**, 30229, doi:10.1038/srep30229 (2016).

13 Si, F. *et al.* Mechanistic Origin of Cell-Size Control and Homeostasis in Bacteria. *Curr Biol* **29**, 1760-1770 e1767, doi:10.1016/j.cub.2019.04.062 (2019).

14 Harris, L. K. & Theriot, J. A. Relative Rates of Surface and Volume Synthesis Set Bacterial Cell Size. *Cell* **165**, 1479-1492, doi:10.1016/j.cell.2016.05.045 (2016).

15 Fantes, P. A., Grant, W. D., Pritchard, R. H., Sudbery, P. E. & Wheals, A. E. The regulation of cell size and the control of mitosis. *J Theor Biol* **50**, 213-244, doi:10.1016/0022-5193(75)90034-x (1975).

16 Kjeldgaard, N. O., Maaloe, O. & Schaechter, M. The transition between different physiological states during balanced growth of Salmonella typhimurium. *J Gen Microbiol* **19**, 607-616, doi:10.1099/00221287-19-3-607 (1958).

17 Cooper, S. Cell division and DNA replication following a shift to a richer medium. *J Mol Biol* **43**, 1-11, doi:10.1016/0022-2836(69)90074-6 (1969).